HEAT TRANSFER ENHANCEMENT OF IMPINGEMENT COOLING BY ADOPTING CIRCULAR-RIBS OR VORTEX GENERATORS IN THE WALL JET REGION OF A ROUND IMPINGEMENT JET

K. Takeishi[1] – R. Krewinkel[2] – Y. Oda[3] – Y. Ichikawa[4]

[1]Tokushima Bunri University, Kagawa, Japan, takeishi@fst.bunri-u.ac.jp, [2]MAN Energy Solutions SE, Oberhausen, Germany, robert.krewinkel@man-es.com, [3]Kansai University, Osaka, Japan, oda.y@kansai-u.ac.jp, [4]Mitsubishi Heavy Industries, Ltd., Hyogo, Japan, yuichi_ichikawa@mhi.co.jp (Worked at Osaka University as a Master Course Student).

ABSTRACT

In the near future, when designing and using Double Wall Airfoils, which are will be manufactured by 3D printers, the positional relationship between the impingement cooling nozzle and the heat transfer enhancement ribs on the target plate naturally become more accurate. Taking these circumstances into account, an experimental study was conducted to enhance the heat transfer of the wall jet region of an impingement round jet cooling by installing circular ribs or vortex generators (VGs) in the impingement cooling wall jet region. The local heat transfer coefficient was measured using the naphthalene sublimation method, which utilizes the analogy between heat and mass transfer. As a result, it was clarified within the ranges of geometries and Reynolds-numbers at which experiments were conducted that it is possible to improve the averaged Nusselt number Nu up to 21% for circular ribs and up to 51% for VGs, respectively.

KEYWORDS

GAS TURBINE, IMPINGEMENT COOLING, HEAT TRANSFER ENHANCEMENT, RIBED-ROUGHENED SURFACE, DOUBLE WALL AIRFOIL

NOMENCLATURE

Cp specific heat [kJ/(kg·K)]
D nozzle diameter [mm]
e rib height [mm]
H distance between nozzle and target plate [mm]
h heat transfer coefficient [W/(m²·K)]
h_D mass transfer coefficient [m/s]
Nu Nusselt number [-]
R gas constant of naphthalene [kJ/(kg·K)]
Re Reynolds number based on D [-]
r distance from stagnation point [mm]
r_{rib} radius of a circle-rib [mm]
p_w saturated vapor pressure [Pa]
Pr Prandtl number [-]
Sc Schmidt number [-]
T_w wall temperature [K]
t_e experimental time [s]
x, y, z coordinates [mm]
δ boundary layer thickness [mm]
δ_z naphthalene sublimation thickness [mm]
λ thermal conductivity [W/(k·K)]
θ azimuth [degrees]
ρ density of air [kg/m³]
ρ_s density of naphthalene [kg/m³]

INTRODUCTION

To increase specific thrust and to improve thermal efficiency, the inlet temperature of jet engines and industrial gas turbines tend to increase ever further. Current turbine inlet temperatures of the latest jet engines and industrial gas turbines are operating at the level of 1600 °C to 1700 °C (Hada *et al.*, 2012). For the turbine first stage vane and blade exposed to such a high temperature gas stream, advanced cooling technologies are used to reduce the metal temperature of the components

so that, in combination with the usage of heat resistant super alloys, the metal temperatures can be maintained at a level that safeguards the integrity of the components.

Impingement jet cooling, serpentine flow passages with ribs, pin fin cooling etc. are used as cooling methods for turbine vanes and blades from the perspective of internal cooling. Film cooling is also used for cooling the outer surfaces. Among these cooling methods, as the thermal load increases, the importance of film cooling increases. However, among the internal cooling methods, impingement cooling is widely used, especially for stationary parts, because it is possible to control the heat transfer coefficient locally and globally and attain a more uniform wall temperature.

The heat transfer coefficient of impingement cooling can be controlled by changing the nozzle hole diameter, the nozzle pitch, the distance between the target plate and the nozzle exit etc. For this reason, impingement cooling is widely used as a cooling technique for the mid-chord portion of turbine vanes. The leading and trailing edges demand the use of different cooling techniques, for example showerhead cooling (due to the extreme thermal load) or pin-fin cooling (due to the limited available width), respectively. Impingement cooling has a very high heat transfer coefficient at the stagnation point, but since the flow velocity decreases quadratically away from the stagnation point, this characteristically decreases rapidly. For this reason, in an attempt to improve the heat transfer of impingement cooling, techniques for promoting heat transfer by attaching ribs, dimples, pin fins, etc. on the target plate have been studied more or less regularly in the past.

Sugimoto *et al.* (2007) measured the local heat transfer coefficient distribution with the naphthalene sublimation method. The authors attached ribs with a square cross section to the wall jet region on a target plate, used a two-dimensional jet nozzle and varied the rib height. Their results showed that the averaged heat transfer coefficient on the target plate takes a maximum value when the rib height is the same as the boundary layer thickness of the flow generated by the wall jet. Many other studies have reported on heat transfer enhancement of impingement cooling by attaching ribs to the target surface. Haiping *et al.* (1997) investigated the positional relationship between ribs and impingement nozzles and revealed that the heat transfer coefficient takes the maximum value when the jet impinges in the middle of the ribs. Son *et al.* (2005) proposed a method of enhancing heat transfer by attaching a roughness element consisting of Perspex Hexagonal Rims to the target surface. Spring *et al.* (2012) showed that heat transfer enhancement can be attained even in a state where the cross flow is large, provided the ratio of the height of the rib e to the impingement nozzle diameter D is $e / D = 1$, and the distance from the jet nozzle to the target plate H is $H / D = 3$ with an inline position of the jet. Trabold and Obot (1987) investigated the cross flow effect on the heat transfer of impingement cooling on rib-roughed surfaces. Two of their most important results were that, first, Nu may decrease when turbulators are introduced and, second, turbulators seem to perform best when the crossflow is strongest. Oda and Takeishi (2014) conducted an LES analysis of the impingement jet flow and heat transfer on a target plate with square and circular ribs. They discuss the heat transfer enhancement after the reattachment of the flow behind the ribs and compare their numerical LES- and RANS-results with experimental data. Only LES is capable of catching most experimental phenomena. They state that a rib height of 0.005m, which is close to the boundary layer thickness, yields an optimum heat transfer enhancement.

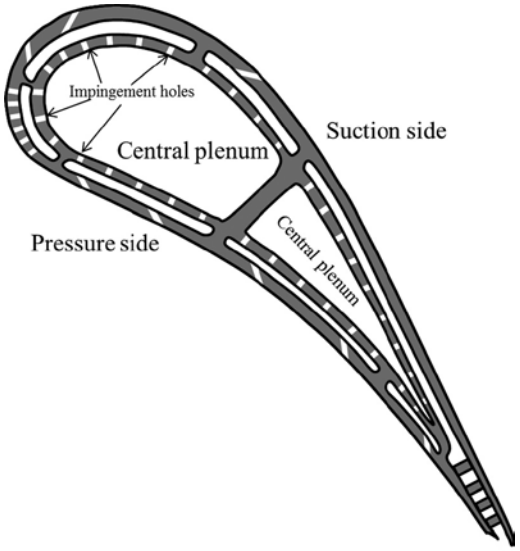

Figure 1: Double wall cooling vane from Li *et al.* (2018)

Currently, a stage is being reached where the cooling structure of the turbine rotating blade can be manufactured using a 3-D printer. When such a

manufacturing method is realized, impingement cooling of the mid-chord of the turbine rotating blade, which has traditionally been difficult, becomes possible. Whether or the improved cooling will be able to counterbalance the foreseeable reduction in material properties compared to, e.g. single-crystal castings, remains to be seen, though. A US Patent (US 7,556,476 B1) describes a cooling structure for double walls. Terzis *et al.* (2014), Stoakes and Ekkad (2011) and Li *et al.* (2018) report on heat transfer research on turbine blades with a double wall cooling structure. Figure 1 shows the cooling structure of a turbine vane with a double wall structure devised by Li *et al.* (2018). The characteristic of the double wall airfoil is that the cooling air used for impingement cooling flows only a relatively short distance through the cavity between the insert and the blade wall and blows out from film cooling holes to the main stream. This cooling structure therefore implies less deterioration in heat transfer performance of the impingement cooling by cross flow. The structure of the double wall airfoil enables impingement cooling for the internal cooling of turbine rotating blades because the insert and the blade wall can be manufactured as one integral part.

When considering a technique for improving the heat transfer performance of impingement cooling applied to a double wall airfoil that can be manufactured with a 3-D printer, the following two aspects are to be taken into account.

* Heat transfer enhancement of the wall jet region with poor heat transfer performance without considering the influence of the cross flow, as this will be weak in double-wall blades.

* A cooling structure manufactured with 3-D printers, making maximum use of features that can very accurately determine the positional relationship between impingement nozzles and heat transfer enhancement ribs.

In this study, based on the above-mentioned considerations, circular ribs and vortex generators (VG) were installed in the wall-jet region of single-hole impingement cooling, and the heat transfer enhancement in the wall-jet region was investigated. Circular ribs are one method of promoting heat transfer utilizing the fact that the heat transfer coefficient of the reattachment point, where a new boundary layer starts, is very high due to the forced separation on the top of the rib and reattachment of the flow. The VG utilizes another effect, namely the heat transfer enhancement effect induced by the strong shear flow caused by the secondary flow it generates.

EXPERIMENTAL METHOD

The distribution of the heat transfer coefficient on the target plate by the impingement jet ejected from the single circular nozzle was measured using the naphthalene sublimation method. A schematic of the experimental apparatus used for the heat transfer experiment is shown in Figure 2. Dry air was supplied from a compressor into the test section through a heat exchanger, a mass flow controller, and a pressure gauge. The test section of the impingement jet heat transfer test apparatus has an entrance section with a mesh screen followed by a contraction section to realize a uniform flow upstream of the impingement jet cooling. The air flows out from a single-hole impingement nozzle. Water at a constant temperature of 20°C, supplied from a constant temperature water circulation device, flows to the heat exchanger and the temperature of the cooling air is thus maintained at 20°C during the experiment.

A target plate is placed relative to the impingement nozzle. The cooling air supply part containing the impingement nozzle is movable so as to change the distance between the nozzle and the target plate. The nozzle plate and the target plate are parallel, and the cooling air strikes the center of the target plate and subsequently flows out of the test section from all sides. The round nozzle diameter is D = 32 mm, the exit of which is orifice-shaped and the distance between the nozzle and the target plate is H/D = 3. The target plate is made of acryl and has a square shape with sides of 400 mm each. A part of the acrylic target plate was cut out and a naphthalene container made of aluminum and measuring 230 mm × 70 mm was attached so as to be level with the target plate surface. The size of the naphthalene within the container is 210 mm × 50 mm, and the naphthalene that was cast into the container was carefully checked to ensure a fully smooth

transition to the surrounding acrylic surface. Two thermocouples that record the temperature of the naphthalene during the test of the impingement cooling are embedded in the aluminum container.

Table 1 shows the dimensions of the circular rib used to enhance the heat transfer by detaching and reattaching the boundary layer flow in the wall jet region. The ribs are of square cross section, with three rib heights e/δ = 0.58, 1.0, 1.42 were prepared with the constant circular rib radius of r/D=3.5. In a second set of tests with the goal of setting the rib height to be the same as the boundary layer thickness δ at the position where the circular rib is installed, heat transfer tests to investigate the effect of the rib location were conducted using five kinds of circular ribs at r/D = 1.6, 2.0, 2.2, 2.5, 3.5 and 4.5 these all maintained the ratio of the rib height e and the boundary layer thickness e/δ= 1.0.

Figure 3 shows the circular ribs and the VG used to enhance heat transfer by attaching them to the wall jet region. The VGs' dimensions are listed in Table 2. As shown in Figure 4, 12 VGs were arranged radially in a 30 ° interval on the target plate around the stagnation point of the impingement jet.

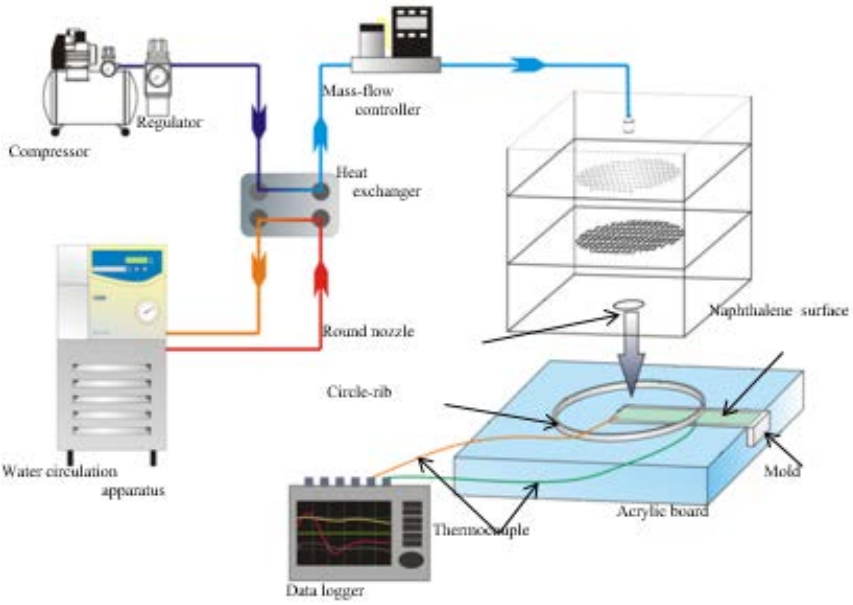

Figure 2: Experimental apparatus

Table 1: Dimensions of circular ribs

Radius of ribs r_{rib} (r_{rib}/D)	Rib height e (e/δ)
51.2 mm (1.6)	1.0 mm (≒1)
61.4 mm (2.0)	1.3 mm (≒1)
70.4 mm (2.2)	1.4 mm (≒1)
89.0 mm (2.5)	1.6 mm (≒1)
112 mm (3.5)	1.3 mm (0.58)
	2.2 mm (≒1)
	3.2 mm (1.42)
144 mm (4.5)	2.9 mm (≒1)

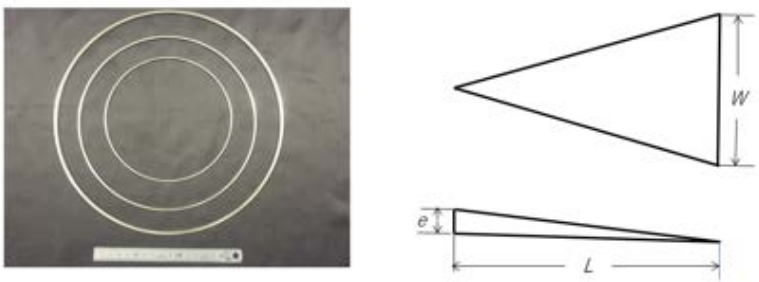

Figure 3: Circular ribs and vortex generator

Table 2: Dimensions of VGs

Length L [mm]	Width W [mm]	Height e [mm]
22	22	1.0
		1.3
		1.6
		1.9
		2.2
		2.9

Naphthalene Sublimation Method

The initial surface profile of the naphthalene was scanned using a two-axis auto-traverse equipment with a resolution of 1μm and a laser displacement sensor, which has a measurement depth of focus ±1 mm with a resolution of 0.1 μm and a linearity error of 0.3%. After the test, which had air blowing onto the surface for 40 to 120 minutes, depending on the fluid temperature and flow velocity (in order to keep the sublimation depth less than 100μm), the surface profile was scanned again. Then, the local naphthalene sublimation depth was calculated as the local change of the surface position from the initial values.

The local mass transfer coefficient is calculated from the following relation:

$$h_d = (RT_w/p_w)\cdot(\rho_s\delta_z/t_e) \qquad (1)$$

where R is the gas constant, T_w is the naphthalene surface temperature, p_w is the saturated vapor pressure of naphthalene in air, ρ_s is the density of solid naphthalene, δ_z is the depth of naphthalene sublimation, and t_e is the flow exposure time. The thermo-physical properties of naphthalene were obtained from Goldstein and Cho (1995). The local mass transfer coefficient can be converted to the local heat transfer coefficient by using the analogy between heat and mass transfer.

$$h = h_d\rho C_p(Sc/\mathrm{Pr})^{1\text{-}n} \qquad (2)$$

where ρ is the density of air, C_p is the specific heat at constant pressure, Sc is the Schmidt number, Pr is the Prandtl number, and n is an empirical constant which is 0.4 in this experiment. This value is in line with Schlünder and Gnielinksi (1967) who take n as 0.42 for the whole region of interest when using naphthalene sublimation and Oda and Takeishi (2015) who state that 0.4 is the correct value for the area between the impingement point and the first rib.

Using the partial derivative method described by Moffat (1988), an uncertainty analysis was performed on the measured values of the local heat transfer coefficient, h, based on uncertainties associated with the measured depth of naphthalene sublimation, naphthalene temperatures, flow rate, and operation time. The precision uncertainties of the naphthalene sublimation depth measured by the laser displacement sensing system, the temperature measured by K-type thermocouples, the flow rate measured by a mass flow controller, and the total operation time were ±0.3%, ±0.1°C, ±0.8%, and ±5 s, respectively. Combining these uncertainties, the total uncertainty of the local heat transfer coefficient, δh, was found to be 5.5–8.3% over a Re_D range of 10,000–70,000.

The area-averaged Nu is calculated by integrating the local Nu distribution.

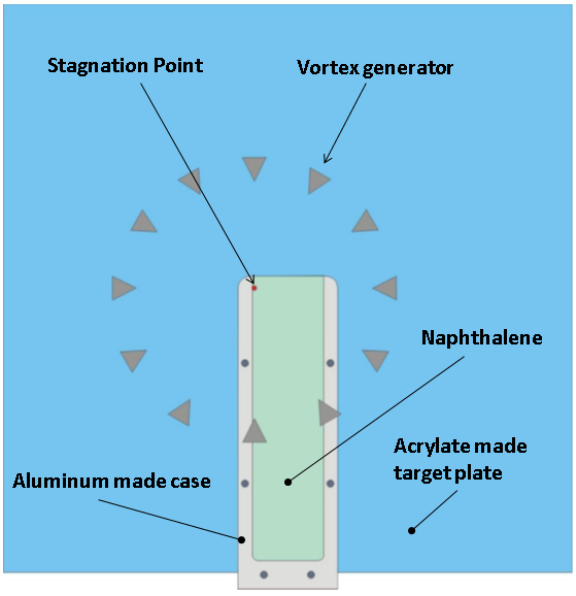

Figure 4: Layout of VGs on the target plate

EXPERIMENTAL RESULTS AND DISCUSSIONS

Effect of the height of the circular ribs on the enhancement of heat transfer

The boundary layer thickness δ in the wall jet region of a circular single jet is measured by a hot wire and empirical equation (3) is established using the measured data.

$$\delta = 0.02r \qquad (3)$$

At the location r / D = 3.5, heat transfer experiments were conducted by changing the height of the circular rib between e/δ = 0.58, 1.0 and 1.42. The experimental conditions are shown in Table 3.

Figure 5 shows the measurement results of the local Nu-distribution in the radial direction using the naphthalene sublimation method under the aforementioned experimental conditions. Figure 6 shows the area-averaged Nu normalized by Nu_0 of the configuration without a circular rib integrated over the whole area of $0 \leqq r/D \leqq 5.6$ with the dimensionless rib height as the parameter on the x-axis. As shown in Figure 6, when the value of the rib height e of the circular rib is about the same as the boundary layer thickness δ at the position where the rib is located, the area-average Nu integrated over the entire surface reaches its maximum value. This is the same result as that of the heat transfer experiments on impingement jets using two-dimensional nozzles which we conducted prior to the current research (Sugimoto *et al.* 2007), which was also confirmed by LES and DNS calculations (Oda *et al.*, 2015). That is, in the state where the flow rate which is blocked by the front face of the rib is smallest, and a forced separating flow on the top of the rib is generated on the upper face of the rib at the outer edge of the boundary layer where the maximum flow velocity is reached. A high heat transfer coefficient on the target plate is achieved where a strong shear flow is generated near the reattachment point.

Table 3: Experimental conditions of circular ribs

Reynolds Number Re_D	10,000
Distance H/D	3.0
Boundary layer thickness δ	2.0
Location of circular ring r/D	3.5
Height of circular rings e/δ	0.58, 1.0, 1.42

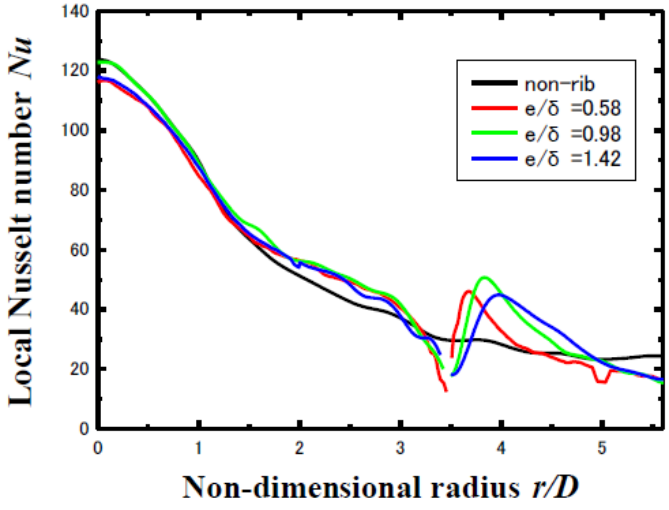

Figure 5: Effect of circular rib height on the local Nu (at the fixed circular rib location of r/D = 3.5)

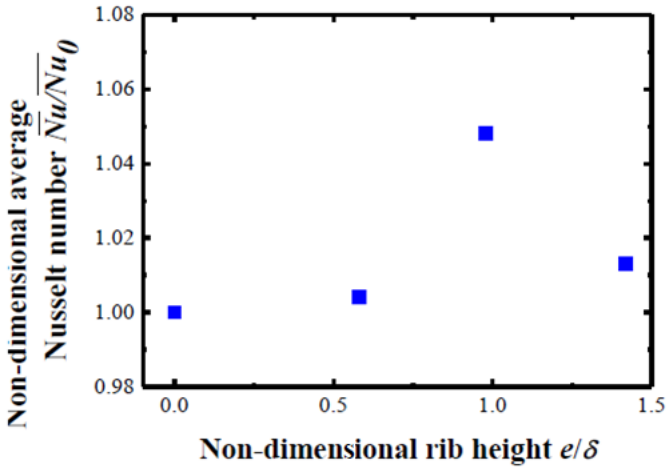

Figure 6: Effect of circular rib height on the averaged Nu (at the fixed circular rib location of r/D = 3.5)

Effect of circular rib location on heat transfer enhancement

In the previous section, it was shown that the area-averaged Nu attains a maximum value when the rib height e of the circular rib coincides with the boundary layer thickness δ at the position where the rib is installed. Based on this result, we conducted experiments aimed at influencing the local heat transfer coefficient by changing the position at which the circular rib was installed, but with the rib height e equal to the boundary layer thickness δ at the point of installation. Table 4 shows the experimental conditions for this set-up.

Figure 7 shows the distribution of the local Nu number that can be achieved by changing the position of the circular rib with a rib height optimized according to our previous discoveries. Although the values for the heat transfer enhancement of ribs just before and just after r/D≈2 fall within the experimental uncertainty, the substantial difference in enhancement after r/D≈2 is well beyond the uncertainty. Again the naphthalene sublimation method was used. Figure 8 shows the results of the calculation of the area-averaged Nu by integrating the measured local Nu-distribution over $0 \leqq r/D \leqq 5.6$. It can be seen from Figure 8 that the area-averaged Nu attains a local maximum near r/D = 2. From Figure 7 it may seem the local Nu reached its maximum when the position of the circular rib is closer to the stagnation point, that is, in the experimental range at r/D = 1.6. However, when the area-averaged Nu is calculated taking the weighted annular area at which the various local Nu are achieved into account, as shown in Figure 8, the maximum Nu is reached near r/D = 2.2. The area-averaged Nu tends to increase with increasing r/D again after a sharp drop immediately after the maximum value around r/D = 2.2. The reason that the area-averaged Nu at r/D = 4.5 is larger than that at r/D = 3.5 is that, although the local Nu at the reattachment point is lower for r/D = 4.5 than for r/D = 3.5, the annular area at r/D = 4.5 is much larger.

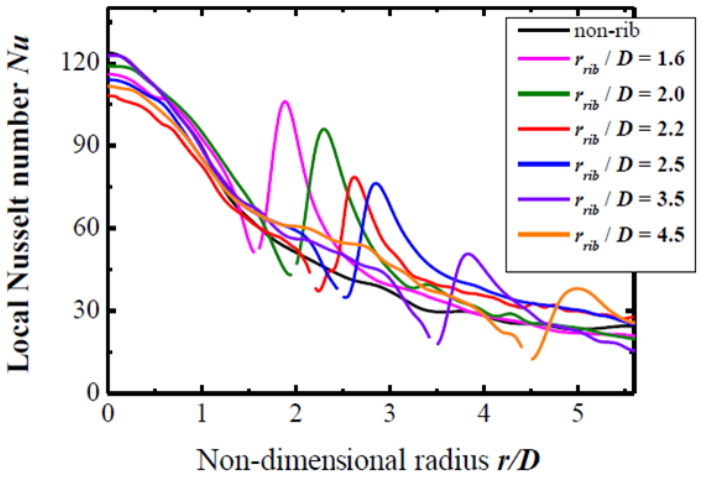

Figure 7: Effect of the circular rib locations on local Nu (at the fixed circular rib height of e/δ = 1.0)

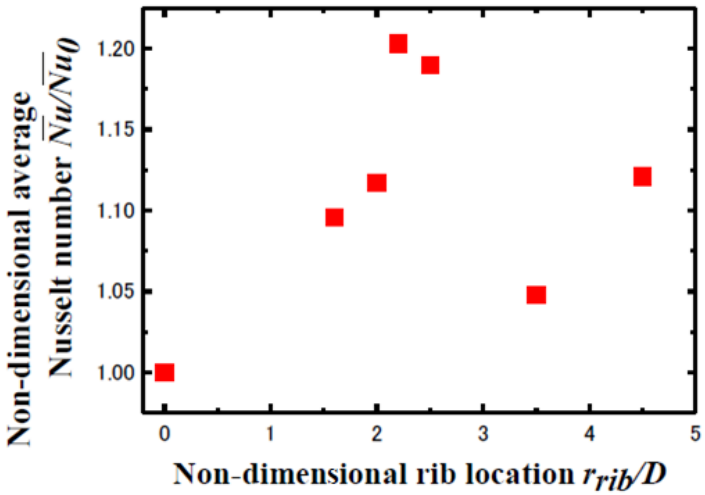

Figure 8: Effect of circular rib location on the averaged Nu (at the fixed circular rib height of e/δ = 1.0)

Table 4: Experimental conditions for locations of circular ribs

Reynolds Number Re$_D$	10,000
Nozzle diameter D	32.0
Distance H/D	3.0
Location of circular ring r/D	1.6, 2.0, 2.2, 2.5, 3.5, 4.5
Height of circular rings e/δ	1.0

Effect of VG on the enhancement of heat transfer

As shown in Figure 4, the experiment was carried out by locating 12 VGs at intervals of 30 degrees around the stagnation point. Figure 9 shows the locations in the set-up where the naphthalene substrate and VG for measuring the local heat transfer coefficient distribution are installed. The measurement of the distribution of the local heat transfer coefficient was conducted within the fan shaped area of 0 ° to 15 ° indicated in Figure 9.

In addition to investigating the influence of the rib height of the circular rib on heat transfer, the influence of the height of the VG on the heat transfer was investigated as well.

Table 5 shows the experimental conditions aimed at examining this influence. In the experiment, using the VG whose shape is shown in Figure 3, the local heat transfer coefficient is measured by the naphthalene sublimation method. The ratio e/δ with the boundary layer thickness δ at the position where the VG is installed, and the height e of the VG were used to define the dimensionless height of the ribs.

The area-averaged Nu was calculated from the integration of the local Nu. Figure 10 shows the distribution of the local Nu measured by the naphthalene sublimation method with $e/\delta = 0$ (i.e. no VG) to 1.38 at $r/D = 2.5$. The distribution of the local Nu number measured along the boundary line between the VGs shown in Figure 9 is depicted in Figure 11. Furthermore, the area-averaged Nu was calculated over 0 to 15 degrees, at $r/D = 0$ to 5.63, i.e the whole measurement area in Figure 9 and this result is shown in Figure 12.

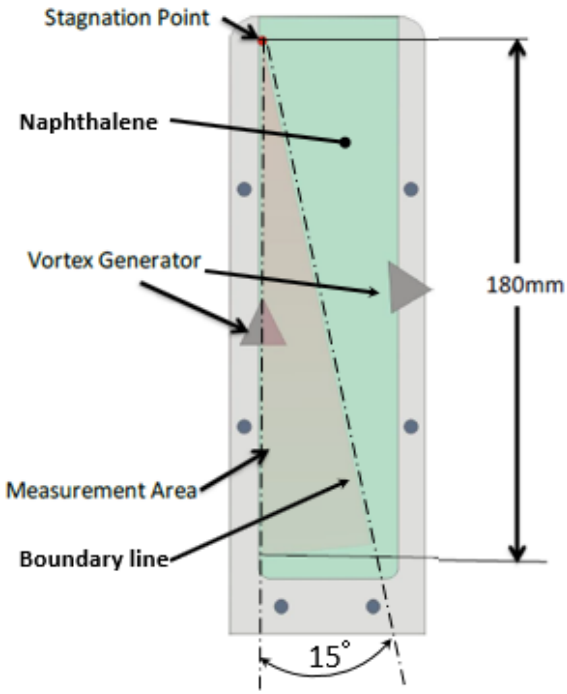

Figure 9: Location of VGs on the naphthalene made target plate

As can be concluded from Figure 10, heat transfer is promoted by the vortex flow generated by the VG. Since this is a three-dimensional flow, the trend of the Nu-boundary line between the VGs cannot be predicted. However, it was clear that heat transfer was promoted by the VG installed at $r/D = 2.5$. Although the effect of promoting high heat transfer is confirmed at $e/\delta = 1.0$, the effect of the VG is worse at $e/\delta = 1.19$. Surprisingly, a high heat transfer enhancement effect was again observed with $e/\delta = 1.38$. It is assumed that for $e/\delta = 1.19$ the swirling flow generated by the VG does not come into contact with the target plate and the swirling flow does thus not contribute to the heat transfer enhancement by reattachment to the target plate.

As shown in n Figure 12, when $e/\delta = 1.0$, the area-averaged value of Nu reaches its maximum value. Therefore, the influence of the VG on the local heat transfer coefficient was investigated using the installation position of the VG as a parameter while keeping the height e of the VG at the

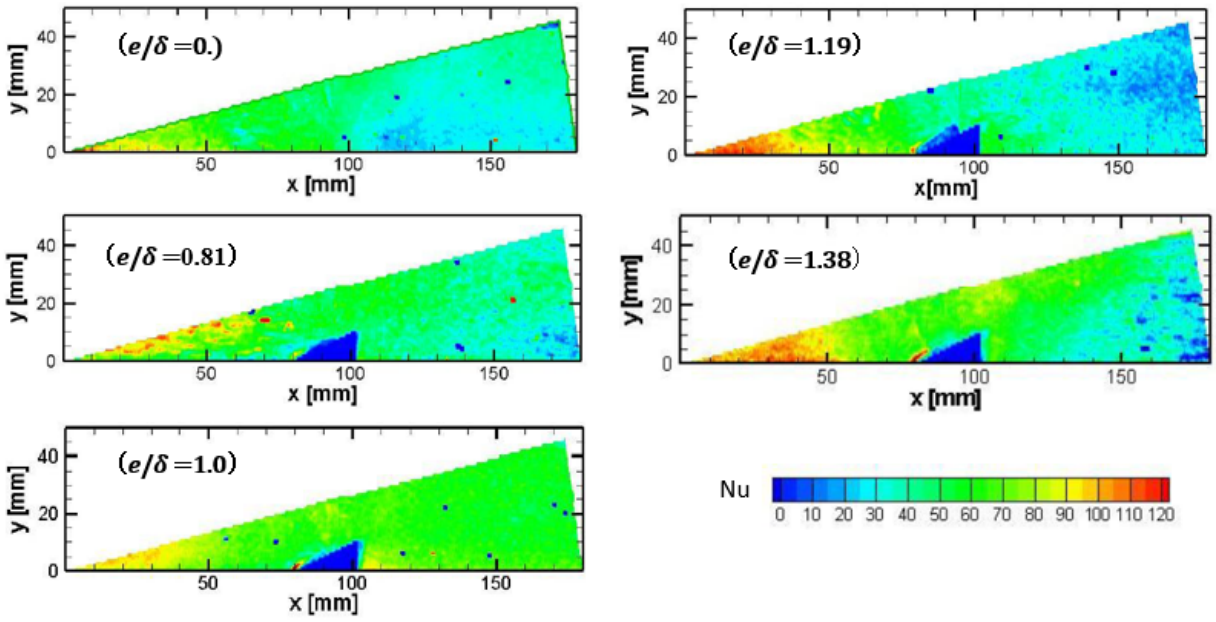

Figure 10: Effect of VG height on the Nu-distribution (at the fixed VG location r/D = 2.5, Re_D = 10,000

installation position at e/δ = 1.0. shows the experimental conditions for investigating the influence of the position of the VG on local Nu. Figure 13 shows the results for the distribution of local Nu on the boundary line between the VGs. The ratio of Nu/Nu_0 is shown in Figure 14. Again, Nu is integrated from the local Nu-distribution with θ = 0 ° to 15 °, r/D = 0 to 5.63, and Nu_0 is the area-averaged value in the same region to which no VG is added. It is difficult to determine the exact location of r/D where Nu/Nu_0 reaches its maximum value because of the small amount of data, but from Figure 14 it is obvious that when the position of the VG is near r/D = 2.5, the averaged Nu takes a local maximum. This tendency is the same as Nu/Nu_0 taking the maximum value near r / D = 2.2 when using the position as a parameter for the circular rib as shown in Figure 8.

Table 5: Locations of VG

Reynolds Number Re_D	10,000
Nozzle diameter D	32.0
Distance H/D	3.0
Location of VG's r/D	1.5, 2.0, 2.5, 3.5, 4.5
Height of VG's e/δ	1.0

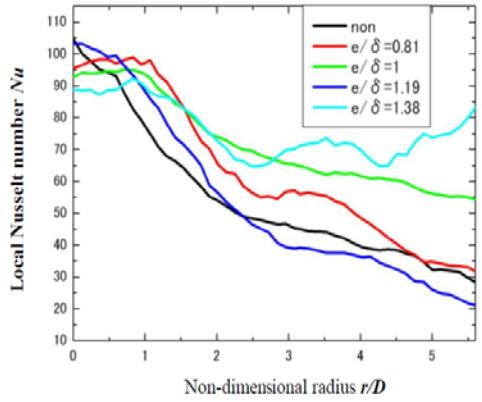

Figure 11: Effect of VG height on the local Nu distribution along boundary line in Fig. 9 (fixed VG location: r/D = 2.5)

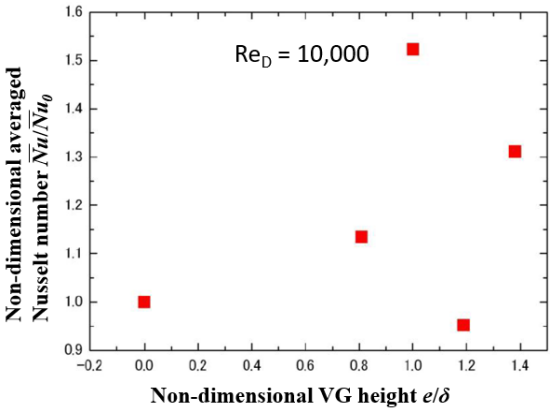

Figure 12: Effect of VG height on the averaged Nu (fixed VG location: r/D = 2.5)

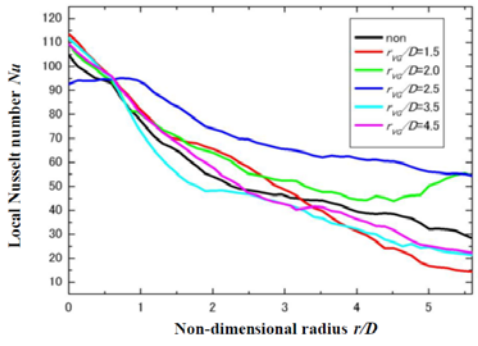

Figure 13: Effect of VG location on the local Nu distribution along boundary line in Fig. 9 (fixed VG height: e/δ = 1.0)

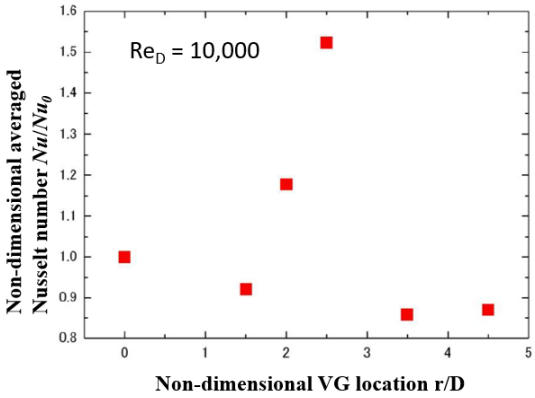

Figure 14: Effect of VG location on the averaged Nu (fixed VG height: e/δ = 1.0)

CONCLUSIONS

A study aimed at enhancing heat transfer in the wall jet region of impingement jet cooling that is suitable for adoption in future double wall airfoils was conducted. The local heat transfer coefficient distribution was measured using the naphthalene sublimation method. The following conclusions can be drawn from the investigation of the heat transfer enhancement effect of circular ribs or VG in the wall jet region of such jets.

1. If the rib height e of the circular rib is set to be about the same as the boundary layer thickness δ, the heat transfer coefficient reaches a maximum.

2. A rib with a height approximately equal to the boundary layer thickness and at a position where $r / D = 2.2$ leads to a local maximum value of the averaged Nu.
3. When VGs are arranged radially around the stagnation point and heat transfer enhancement is investigated by changing the VG height, then the configuration with e $/\boldsymbol{\delta} = 1.0$ and $r / D = 2.5$ achieves a global maximum. This trend is similar to that of the circular ribs.
4. Within the range of the experiments, it was possible to improve the area-averaged Nu with up to 21% for circular ribs and up to 51% for VGs. Although VG may have little effect in some cases, with the right set of parameters it constitutes a means of effective heat transfer enhancement.
5. In future impingement cooling structures which can be manufactured using AM, such as double wall airfoils, the positional relationship between the impingement nozzle and features such as the heat transfer enhancement rib on the target surface is fixed. The research discussed in this study provides a very useful way of thinking of new ways to design impingement cooling for double wall airfoils.

REFERENCES

Goldstein, R. J., and Cho, H. H., (1995), *A Review of Mass Transfer Measurements Using Naphthalene Sublimation*, Exp. Therm. Fluid Sci., 10, pp. 416‑434.

Hada, S., Yuri, M., Masada, J., Ito, E., and Tsukagoshi, K., (2012), *Evolution and Future Trend of Large Frame Gas Turbines a New 1600 Degree C, J Class Gas Turbine*, Proc. ASME Expo 2012, Paper No. GT2012-68574.

Haiping, C., Dalin, Z., and Taiping, H., (1997), *Impingement Heat Transfer from Rib Roughened Surface within Arrays of Circular Jets: The Effect of the Relative Position of the Jet Hole to the Ribs*, Proc. ASME Expo 1997, Paper No. 97-GT-331.

Li, W., Li, X., Ren J., and Jiang, H., (2018), *A Novel Method for Designing Fan-Shaped Holes With Short Length-to-Diameter Ratio in Producing High Film Cooling Performance for Thin-Wall Turbine Airfoil*, J. of Turbomachinery, 140 (9), pp. 091004.

Moffat, R. J., (1988), *Describing the Uncertainties in Experimental Results*, Experimental Therm. Fluid Science, 1, pp. 3-17.

Oda, Y., and Takeishi, K., (2014), *Concurrent Large-Eddy Simulation of Wall-Jet Heat Transfer Enhanced by Systematically-Deformed Turbulence Promoter*, Proc. IHTC-15, Kyoto.

Schlünder, E.U., and Gnielinski, V., (1967) *Wärme- und Stoffübertragung zwischen Gut und aufprallendem Düsenstrahl*, Chemie-Ing.-Techn., 39 (9/10), pp. 578-584.

Son, C., Dailey, G., Ireland, P., and Gillespie, D., (2005), *An Investigation of the Application of Roughness Elements to Enhance Heat Transfer in an Impingement Cooling System*, Proc. ASME Turbo Expo 2005, Paper No. GT2005-68504.

Spring, S., Xing, Y., and Weigand, B., (2012), *An Experimental and Numerical Study of Heat Transfer from Arrays of Impinging Jets With Surface Ribs*, ASME. J. Heat Transfer, 134(8), pp. 082201-1.

Stoakes P., Ekkad, S., (2011), *Optimized Impingement Configurations for Double Wall Cooling Applications*, Proc. ASME Turbo Expo 2011, Paper No. GT2011-46143.

Sugimoto, S., Takeishi, K., Oda, Y., and Harada, T., (2007), *A Study on Heat Transfer Enhancement of Jet Impingement Cooling by Turbulence Promotors*, Proc. IGTC2007, TS-116.

Terzis, A., Cochet, M., von Wolfersdorf, J., Weigand B., and Ott, P., (2014), *Detailed Heat Transfer Distributions of Narrow Impingement Channels With Varying Jet Diameter*, Proc. ASME Turbo Expo 2014, Paper No. GT2014-25910.

Trabold, T. A., and Obot, N. T., (1987), *Impingement Heat Transfer Within Arrays of Circular Jets. Part II: Effects of Crossflow in the Presence of Roughness Element*, Proc. of the International Gas Turbine & Aeroengine Congress & Exhibition, Anaheim, California, Paper No. 87-GT-200.

Liang, G., (2009), *Turbine Airfoil with Multiple near Wall Compartment Cooling*, US Patent 7,556,476 B1, Date of Patent: Jul. 7, 2009.